Applied and Environmental Microbiology, June 2008, p. 3497–3511 Vol. 74, No. 11
0099-2240/08/$08.00+0 doi:10.1128/AEM.02844-07

Investigating the Properties of *Bacillus thuringiensis* Cry Proteins with Novel Loop Replacements Created Using Combinatorial Molecular Biology▽†

Craig R. Pigott,* Martin S. King,‡ and David J. Ellar

Department of Biochemistry, University of Cambridge, 80 Tennis Court Road, Cambridge CB2 1GA, United Kingdom

Received 17 December 2007/Accepted 4 April 2008

Cry proteins are a large family of crystalline toxins produced by *Bacillus thuringiensis*. Individually, the family members are highly specific, but collectively, they target a diverse range of insects and nematodes. Domain II of the toxins is important for target specificity, and three loops at its apex have been studied extensively. There is considerable interest in determining whether modifications in this region may lead to toxins with novel specificity or potency. In this work, we studied the effect of loop substitution on toxin stability and specificity. For this purpose, sequences derived from antibody complementarity-determining regions (CDR) were used to replace native domain II apical loops to create "Crybodies." Each apical loop was substituted either individually or in combination with a library of third heavy-chain CDR (CDR-H3) sequences to create seven distinct Crybody types. An analysis of variants from each library indicated that the Cry1Aa framework can tolerate considerable sequence diversity at all loop positions but that some sequence combinations negatively affect structural stability and protease sensitivity. CDR-H3 substitution showed that loop position was an important determinant of insect toxicity: loop 2 was essential for activity, whereas the effects of substitutions at loop 1 and loop 3 were sequence dependent. Unexpectedly, differences in toxicity did not correlate with binding to cadherins—a major class of toxin receptors—since all Crybodies retained binding specificity. Collectively, these results serve to better define the role of the domain II apical loops as determinants of specificity and establish guidelines for their modification.

Bacillus thuringiensis encompasses a group of aerobic, gram-positive spore-forming bacteria that produce large crystalline inclusions consisting of entomocidal protein toxins (67). Cry toxins are a major constituent of these inclusions and the screening of thousands of *B. thuringiensis* strains has revealed that these proteins comprise a large family of related toxins with diverse specificities. The majority are toxic toward lepidopterans (butterflies and moths), dipterans (flies and mosquitoes), and coleopterans (beetles) (67), but some Cry toxins have been reported to kill hymenopterans (wasps and bees) (27) and nematodes (52, 78). Comparative sequence analyses have revealed five blocks of conserved amino acids found in most toxins (31) and that toxin genes typically encode proteins of 130 to 140 kDa or approximately 70 kDa. Phylogenetic analyses have shown a correlation between sequence similarity and insect order specificity (9, 17).

Cry toxin protein inclusions must be activated to be functional (67). In lepidopterans, this multistep process starts when crystals are ingested by susceptible larvae. The high pH of the midgut promotes crystal solubilization and the release of protoxins. This exposes protoxin cleavage sites that are cut by host proteases to release the activated core. The toxin then binds to receptors on the surface of the midgut epithelium (as reviewed by Pigott and Ellar [61]), where it is generally accepted that they oligomerize and insert into the membrane, although alternative models have recently been proposed (86, 87). The action of the toxin disrupts the membrane and allows ions and water to enter the cell, leading to swelling, lysis, and eventually the death of the host (42).

The structures of several Cry toxins—including Cry1Aa (30), Cry1Ac (21, 47), Cry2Aa (55), Cry3Aa (48), Cry3Ba (26), Cry4Aa (8), and Cry4Ba (7)—have been solved by X-ray crystallography. Despite differences in their primary sequences and insect specificities, all toxins have been found to share a similar three-domain structure (Fig. 1). Domain I consists of an α-helical bundle of six amphipathic helices that surround an inner hydrophobic helix. Biophysical and mutational analyses suggest that this domain undergoes a conformational change at the membrane surface that leads to insertion and pore formation (47, 53, 59, 65, 72, 73). Domain II is described as a β-prism and consists of three antiparallel β-sheets. Its structure is the most variable of the three domains, particularly at its apex, where three loops implicated in receptor binding (64) differ considerably in their length and conformation (7). Domain III has a β-sandwich structure formed by two antiparallel β-sheets and has also been implicated in receptor binding (11, 16, 34, 35, 45).

Receptor interactions are an important determinant of Cry toxin specificity, and the identification and validation of putative receptors have been a major focus of Cry toxin research (61). Lepidopteran receptors are the best characterized, and most work has focused on the aminopeptidase N and cadherin-

* Corresponding author. Present address: Department of Biochemistry and Molecular Biology, University of British Columbia, 2350 Health Sciences Mall, Vancouver, BC V6T 1Z3, Canada. Phone: (604) 822-3178. Fax: (604) 822-5227. E-mail: c.r.pigott.02@cantab.net.

‡ Present address: MRC Dunn Human Nutrition Unit, Wellcome Trust/MRC Building, Hills Road, Cambridge CB2 0XY, United Kingdom.

† Supplemental material for this article may be found at http://aem.asm.org/.

▽ Published ahead of print on 11 April 2008.

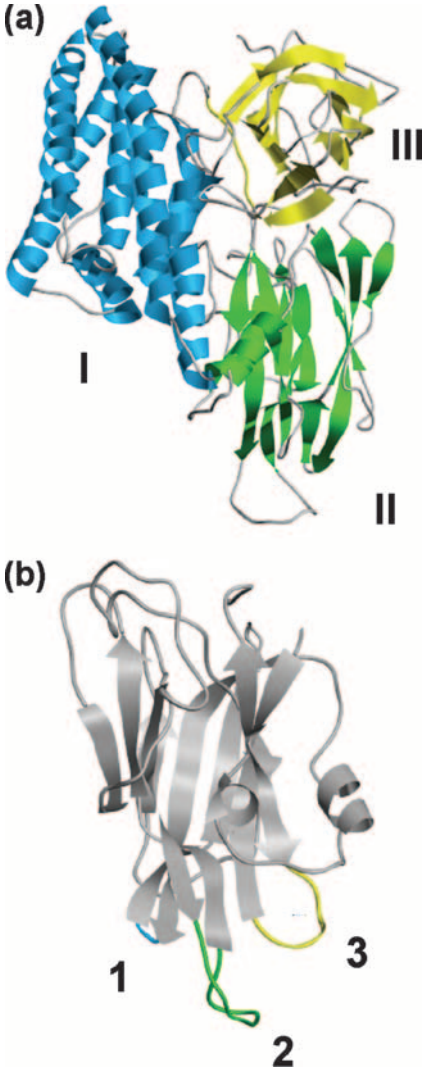

FIG. 1. The structure of Cry1Aa (30) (PDB code 1CIY) highlighting the three domains of the active toxin (a) and the three apical loops of domain II (b). The molecular graphic images were produced using the UCSF Chimera package (60) from the Resource for Biocomputing, Visualization, and Informatics at the University of California, San Francisco (supported by NIH P41 RR-01081).

like receptors. Aminopeptidase N receptors were the first to be discovered (41, 66), and 38 members in 5 different classes have been described, many of which have been shown to bind to Cry toxins and to enhance pore formation in vitro (51, 68). Cadherin-like receptors have also been shown to bind to Cry proteins, and their expression in cultured cells confers toxin susceptibility (22, 23, 33, 39, 71, 86). Furthermore, disruptions to the cadherin gene have been implicated in insect resistance (25, 54, 83). The precise role and importance of each receptor family in mediating toxicity in vivo are currently a matter of debate, and several models have been proposed (10, 38, 86).

Traditionally, the development of Cry toxin-based biopesticides has relied on the screening of natural isolates of *B. thuringiensis* for toxins with activity toward target pests. This approach has led to the identification of many Cry toxins used to control medically and agriculturally important pests (67); however, in many cases, screening efforts have failed to identify Cry toxins specific for a desired organism (19, 79). While screening will likely continue to identify toxins with new specificities, our increasing understanding of the determinants of Cry toxin specificity suggests that protein engineering coupled with phage display technology (76) may become a viable alternative.

Several groups have made modifications to the specificity-determining regions of Cry toxins in an attempt to increase potency or develop completely novel specificities. de Maagd et al. (18) used in vivo recombination to create a series of Cry1Ab and Cry1Ca hybrids. One hybrid, consisting of domains I and II of Cry1Ab and domain III of Cry1Ca, was found to be greater than 60-fold more toxic than Cry1Ab (50% lethal concentration, >100 μg/g) and greater than 6-fold more toxic than Cry1Ca (50% lethal concentration, 11 μg/g) to *Spodoptera exigua* larvae. An expanded collection of hybrids containing domains I and II from Cry1Ac, Cry1Ba, Cry1Ea, or Cry1Fa and domain III from Cry1Ca also showed enhanced toxicity toward *S. exigua*, demonstrating the importance of domain III as a specificity determinant for this insect (20). Additional protein engineering studies have focused on enhancing toxicity by mutating the domain II loops. Rajamohan et al. (62) introduced point mutations into loop 2 of Cry1Ab and created a toxin 36-fold more active against *Lymantria dispar* larvae with an 18-fold increased binding affinity for brush border membrane vesicles (BBMV). Wu et al. (81) mutated three residues in loop 1 of Cry3Aa and found an 11-fold increase in toxicity to *Tenebrio molitor*. More recently, loop swapping has been utilized to modulate toxin specificity. Cry4Aa, but not Cry4Ba, is toxic to the mosquitoes *Culex quinquefasciatus* and *Culex pipiens*. By remodeling the domain II loops of Cry4Ba to resemble Cry4Aa, toxicity to *C. quinquefasciatus* and *C. pipiens* increased by more than 285- and 700-fold, respectively (1). In a similar study, Cry19Aa, a mosquitocidal toxin with specificity toward *Anopheles stephensi* and *C. pipiens* but with no measurable activity against *A. aegypti*, was made more than 42,000-fold more toxic to *A. aegypti* by engineering putative domain II loops 1 and 2 to resemble that of Cry4Ba (2). Liu and Dean (49) introduced mosquitocidal activity to Cry1Aa by making modifications to the sequence of loops 1 and 2 based on a sequence alignment with Cry4Ba, a naturally occurring mosquitocidal toxin. Overall, these results serve to indicate the potential of protein engineering to expand the utility of naturally occurring Cry toxins.

In other fields, protein engineering has been used extensively to introduce novel binding specificities into protein scaffolds. Both rational and combinatorial approaches have been used with a variety of structurally diverse scaffolds (4, 5, 32). Antibodies are perhaps the best studied of all protein scaffolds and affinity transfer by complementarity determining region (CDR) loop swapping has become routine (37). Loop swapping has also been used to generate synthetic antibody libraries with CDR combinations not found in nature (69). Such libraries have been screened against haptens, peptides, carbohydrates, and proteins, and antibodies with dissociation constants in the subnanomolar range have been identified. Affinity transfer by CDR replacement has even been successful with non-immunoglobulin scaffolds. Nicaise et al. (57) grafted the third CDR of a lysozyme-specific camel antibody onto a neocarzi-

nostatin and found that the hybrid specifically bound to lysozyme.

In many ways, Cry toxin domain II is similar to the variable domain of an antibody. The antibody variable domain is a compact globular structure composed of two antiparallel β-sheets formed from nine β-strands (58). Domain II is formed by three antiparallel β-sheets packed together to form a β-prism with pseudo threefold symmetry (48). In both cases, apex loops are involved in receptor/antigen interactions and are highly variable in length, sequence, and conformation.

Based on the success of previous Cry toxin engineering studies, an increasing knowledge of toxin mechanisms of action, and the structural and functional similarities between Cry toxin domain II and the antibody variable domain, we reasoned that antibody CDR sequences might be used to expand the diversity of Cry toxins through domain II loop replacement. In particular, it was of interest to determine whether the third heavy-chain CDR (CDR-H3), the most variable of the six CDRs that form the antigen binding site, could be integrated into the domain II framework of Cry1Aa. The ultimate goal was to create a large library of Cry toxin–CDR-H3 fusions, or "Crybodies," containing variants with binding specificity for a wide range of targets. Such a library could be used to generate toxins capable of targeting insects for which there is no existing Cry toxin treatment or to create entirely novel toxins useful in medical applications. This paper presents the design, construction, and analysis of a set of Crybodies to determine the feasibility of such an approach.

MATERIALS AND METHODS

Library assembly. Libraries of Crybodies were constructed in three steps (Fig. 2). First, CDR-H3 sequences were recovered from the human single-chain variable fragment (scFv) antibody library CAT DP47 (a generous gift from Cambridge Antibody Technology Limited). Phage DNA was PCR amplified using primers CDf and DP47r (the sequences of all the oligonucleotides used in this study can be found in the supplemental material) to yield products encoding CDR-H3 sequences (Fig. 2c). Digestion with the restriction endonuclease BpmI cut the amplified products once to release upstream antibody framework sequences. Fragments encoding CDR-H3 were then isolated and ligated to synthetic double-stranded DNA toxin adaptors with 2-bp single-stranded DNA extensions designed to match the BpmI-digested CDR-H3 fragments. This method of joining resulted in an extra "adaptor" codon, encoding glycine, between the toxin framework and the CDR-H3 sequence (Fig. 2b). The toxin adaptors L1, L3, and L5 corresponded in sequence to *cry1Aa13* immediately upstream of loop 1, loop 2, and loop 3, respectively. Next, the products of ligation were PCR amplified with the toxin framework primers A1fl, A2fl, or A3fl, and the antibody framework primers CDr-1, CDr-2, CDr-3, and CDr-4. Sequence variability downstream of the CDR-H3 loop necessitated the use of four degenerate primers to permit the amplification of all antibody library variants. As a result of amplification, a BpmI restriction site was introduced that permitted the release of downstream antibody framework sequences following restriction digestion. Fragments encoding the CDR-H3 sequences were subsequently isolated, ligated to the appropriate toxin adaptor fragment (L2-1,2; L4-1,2; or L6-1,2), and then amplified with the corresponding primer set (A1f/A1r, A2f/A2r, or A3f/A3r) to create A1, A2, or A3. To increase library diversity, the adaptor codons were designed to encode a cysteine residue (L2-1, L4-1, or L6-1) or a tryptophan residue (L2-2, L4-2, or L6-2) at this junction (Fig. 2b).

The second step of the library assembly involved PCR amplification of *cry1Aa13* framework sequences around each of the apical loops of domain II. These sequences served as templates to position each CDR-H3 sequence correctly in the toxin framework. As shown in Fig. 2c, four fragments (I, II, III, and IV) were required for the assembly of cc123. Fragment I was amplified from *cry1Aa13* with the primer set CP4/Ir, fragment II with IIf/IIr, fragment III with IIIf/IIIr, and fragment IV with IVf/CP5. The framework fragments required for the assembly of the other six Crybody libraries depended on the domain II loop or a combination of loops omitted from the replacement. For example, fragments I and II-IV were required for the assembly of the cc1 library, the latter fragment generated by PCR amplification of *cry1Aa13* with primers IIf and CP5.

The third and final stage of the library assembly involved a series of overlap extension PCR amplifications to join together the recovered CDR-H3 fragments and the toxin framework sequences. The cc123 library was built by joining three DNA fragments per PCR. To create IA1II, fragments I, A1, and II were combined and subjected to six rounds of thermocycling without primers to generate IA1II. The production of IA1II was made possible by the 60 bp of sequence identity shared between I and A1 and between A1 and II. IA1II was subsequently amplified with primers CP4 and IIr following additional rounds of PCR. The fragment IIIA3IV was created by a similar method and involved the union of fragments III, A3, and IV followed by amplification with the primer set IIIf/CP5. To complete the assembly of the cc123 library, fragments IA1II, A2, and IIIA3IV were joined and then amplified with primers CP4 and CP5. The remaining six Crybody libraries were created by a similar method, except that the fragments joined depended on the domain II loop or a combination of loops omitted from the assembly. For example, the cc1 library was assembled by combining fragments I, A1, and II-IV and amplifying the resulting template with primers CP4 and CP5.

Cassettes were restriction digested with XhoI and BamHI and ligated to the vector backbone of plasmid pCP0, a derivative of the *B. thuringiensis*/*Escherichia coli* shuttle vector pSVP27A (15) that expresses a modified form of the *cry1Aa13* gene with novel XhoI and BamHI restriction sites. Plasmids were sequenced with primers CP4 and CP5, and those encoding Crybodies with uninterrupted open reading frames were subsequently used to transform *B. thuringiensis* IPS 78/11 (77) using the method of Bone and Ellar (6).

Analysis of crystal formation. Strains of *B. thuringiensis* IPS 78/11 were incubated at 30°C for 48 h on acid casein hydrolysate-enzymatic casein hydrolysate-enzymatic yeast extract (CCY) agar (70) with 6 μg/ml chloramphenicol to induce sporulation and the production of crystalline Crybody inclusions. Crystal formation was assessed by observing isolated colonies by phase contrast microscopy.

Toxin solubilization and activation. Isolated colonies of *B. thuringiensis* IPS 78/11 expressing Crybodies were used to inoculate 5-ml cultures of CCY agar supplemented with 6 μg/ml chloramphenicol. Cultures were grown under aerobic conditions at 30°C in an orbital incubator (200 rpm) for 48 h or until complete sporulation was observed by phase contrast microscopy. Cultures were then centrifuged at 9,820 × *g* for 10 min at 4°C. The resulting pellets were resuspended in 1 ml of 0.5 M NaCl and transferred to microcentrifuge tubes. Cell suspensions were then centrifuged at 13,400 × *g* for 5 min at 4°C. Supernatants were discarded and the pellets resuspended in 1 ml of MilliQ water. Centrifugation was repeated and the final pellet resuspended in 50 μl MilliQ water.

Crybody inclusions were solubilized in freshly prepared buffer containing 50 mM Na_2CO_3 (pH 9.6) and 10 mM dithiothreitol for 1 h at 37°C. The samples were subsequently centrifuged at 13,400 × *g* for 10 min, and the soluble fractions were isolated.

To test protease sensitivity, solubilized Crybodies were neutralized with 0.2 M Tris-HCl (pH 7.0) and then digested with 0.2 mg/ml trypsin for 30 min at 37°C.

Bioassays. The toxicity of Crybodies toward *Manduca sexta* neonates was assessed as described previously (28) with some modifications. Strains of *B. thuringiensis* IPS 78/11 expressing wild-type Cry1Aa13 or a Crybody were cultured in CCY medium supplemented with 6 μg/ml chloramphenicol until complete sporulation was observed by phase contrast microscopy (48 to 72 h). Twenty microliters of each culture was applied to the surface of *M. sexta* diet (3) in 48-well plates. Neonates were added, one per well, and incubated for 5 days, at which point mortality was assessed. Crybodies from libraries cc1, cc2, and cc3 were tested in three independent trials, six insects per trial. Crybodies from libraries cc12 and cc23 were tested twice, six insects per trial.

Binding specificity. An enzyme-linked immunosorbent assay (ELISA) was used to test whether Crybodies could bind to recombinant fragments of the *Heliothis virescens* cadherin-like protein HevCaLP. Plasmids encoding six-His-tagged CAD3 and M1429$^-$ were generously provided by S. Gill (University of California, Riverside) and were expressed and purified as previously described (82). Solubilized crystalline inclusions were prepared and quantitated using the Bio-Rad protein assay. To correct for the presence of contaminating *B. thuringiensis* proteins in the extract, the concentration of protein in a solubilized extract from a crystal-negative strain was subtracted from each toxin concentration. Wells of a 96-well U-bottom Maxisorp microtiter plate (Nunc) were coated with solubilized toxin diluted to 1 μg/ml in phosphate-buffered saline (PBS) (140 mM NaCl, 2.5 mM KCl, 10 mM Na_2HPO_4, 1.75 mM KH_2PO_4 [pH 7.4]) and incubated overnight at 4°C. Negative control wells were coated with a solubilized protein extract from a crystal-negative strain. The next day, the wells were rinsed three times with PBS-T (PBS, 0.05% [vol/vol] Tween 20). The wells were subsequently blocked with BPBS-T (PBS-T, 1% [wt/vol] bovine serum albumin) for

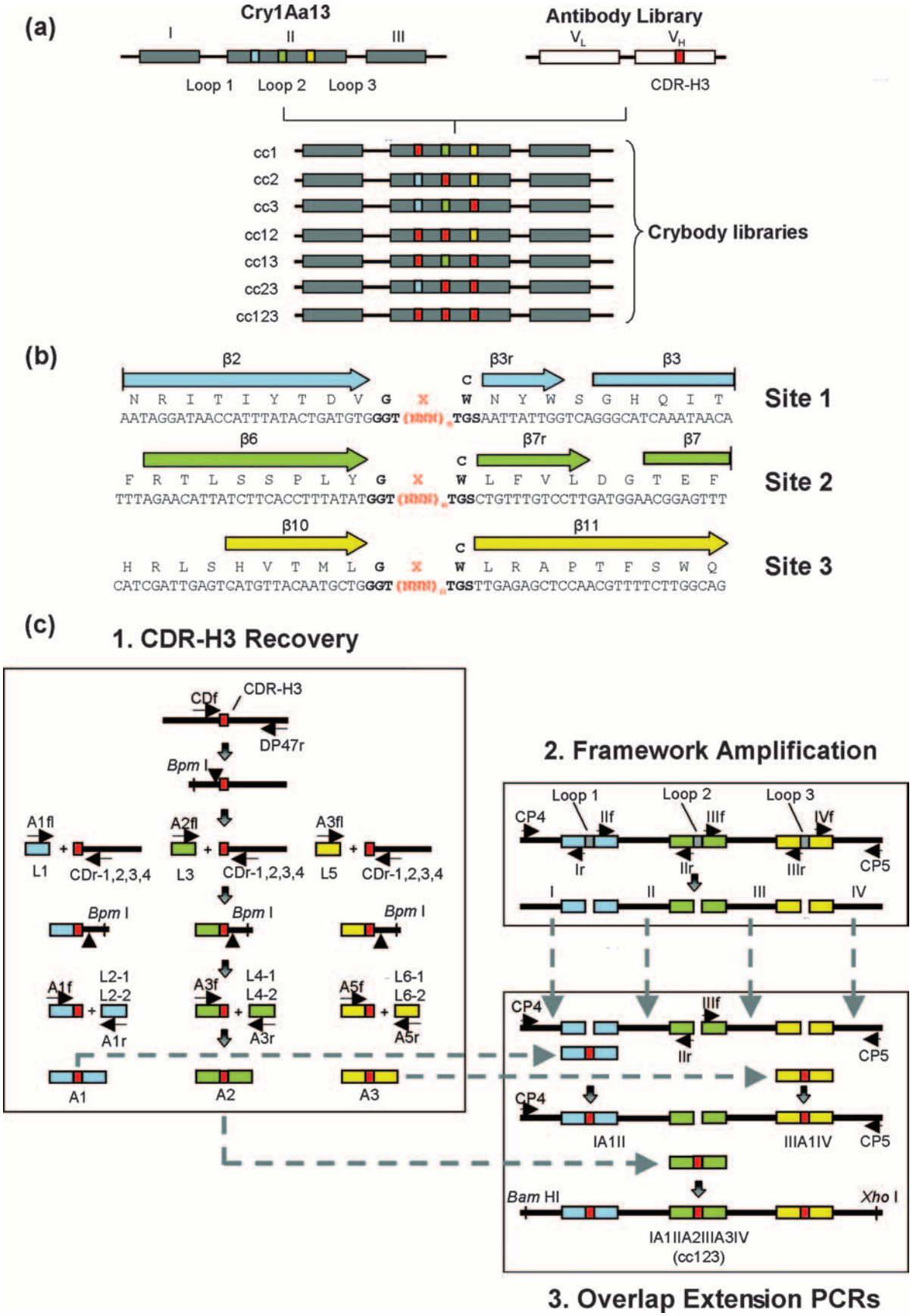
(a)
Cry1Aa13
I
II
III
Loop 1
Loop 2
Loop 3
Antibody Library
V_L
V_H
CDR-H3
cc1
cc2
cc3
cc12
cc13
cc23
cc123
Crybody libraries
(b)
β2
β3r
β3
N R I T I Y T D V G X W N Y W S G H Q I T
AATAGGATAACCATTTATACTGATGTGGGT (NNN)$_n$ TGSAATTATTGGTCAGGGCATCAAATAACA
Site 1
β6
β7r
β7
F R T L S S P L Y G X W L F V L D G T E F
TTTAGAACATTATCTTCACCTTTATATGGT (NNN)$_n$ TGSCTGTTTGTCCTTGATGGAACGGAGTTT
Site 2
β10
β11
H R L S H V T M L G X W L R A P T F S W Q
CATCGATTGAGTCATGTTACAATGCTGGGT (NNN)$_n$ TGSTTGAGAGCTCCAACGTTTTCTTGGCAG
Site 3
(c)
1. CDR-H3 Recovery
CDf
CDR-H3
DP47r
Bpm I
A1fl
A2fl
A3fl
L1
CDr-1,2,3,4
L3
L5
A1f
L2-1
L2-2
A1r
A3f
L4-1
L4-2
A3r
A5f
L6-1
L6-2
A5r
A1
A2
A3
2. Framework Amplification
Loop 1
Loop 2
Loop 3
CP4
IIf
IIIf
IVf
Ir
IIr
IIIr
CP5
I
II
III
IV
IA1II
IIIA1IV
Bam HI
Xho I
IA1IIA2IIIA3IV
(cc123)
3. Overlap Extension PCRs

30 min at room temperature and then washed as before. Next, the wells were coated with BPBS-T or BPBS-T containing 10 μg/ml CAD3 or 10 μg/ml M1429$^-$ for 1 h at room temperature. The wells were washed as before and then coated with a Ni-nitrilotriacetic acid horseradish peroxidase conjugate (Qiagen) diluted 1:1,000 in BPBS-T. After a 1-h incubation at room temperature, the wells were washed as before and then coated with SureBlue TMB one-component microwell peroxidase substrate (KPL). The substrate was allowed to develop for 10 min, at which point the reaction was stopped by adding 1 M HCl. The absorbance was measured at 450 nm using a microtiter plate reader.

Analysis of Crybody binding to *M. sexta* BBMV receptors was carried out by a ligand blot assay. BBMV were isolated from *M. sexta* midguts using the modified method of Wolfersberger et al. (80) described by Carroll and Ellar (12). BBMV protein was resolved by sodium dodecyl sulfate-polyacrylamide gel electrophoresis (SDS-PAGE) and then electrotransferred to nitrocellulose membranes. The blots were then blocked in MTBS-T (25 mM Tris-HCl [pH 7.4], 137 mM NaCl, 2.7 mM KCl, 5% [wt/vol] skimmed-milk powder, 0.05% [vol/vol] Tween 20) washed three times with TBS-T (MTBS-T without skimmed-milk powder) and probed with either activated Cry1Aa13 or Cry1Aa13.2.4D5 in MTBS-T. After being washed, the blots were incubated with anti-Cry1Aa polyclonal antibodies in MTBS-T, washed, and then incubated with anti-rabbit IgG antibodies conjugated to horseradish peroxidase. The blots were developed using an ECL kit (Amersham) according to the manufacturer's instructions.

Construction and analysis of CryMK.123. CryMK.123 was constructed to determine whether the domain II loops of Cry1Aa13 were required for cadherin binding. Synthetic complementary pairs of oligonucleotides (see the supplemental material) were designed to contain the desired loop modifications flanked by 20 to 30 bp of sequence identical to the framework region around the natural toxin loops. Fragments I, II, III, and IV were joined to the oligonucleotide pairs in a series of overlap extension PCRs similar to that used for Crybody construction. The resulting cassette was digested with XhoI and BamHI and ligated to pCP0.

Binding studies were carried out using solubilized, activated Cry1Aa13 or CryMK.123 purified from cultures of *B. thuringiensis* strain IPS 78/11. Briefly, cultures were grown in CCY broth supplemented with 6 μg/ml chloramphenicol for 48 h at 30°C to induce sporulation and crystal production. Following the centrifugation of the cultures at 8,000 × *g* for 30 min, the supernatant was discarded and the pellet washed three times (0.01% [vol/vol] Triton X-100, 50 mM NaCl, and 50 mM Tris-HCl [pH 8.5]). The crystals were solubilized and activated as described previously. Toxin samples were filtered through a 0.22-μm filter and loaded onto a 1-ml HiTrap Q Sepharose anion-exchange column (GE Healthcare) equilibrated with $NaHCO_3$ buffer (pH 9.5). The toxin was eluted with a 0 to 1 M NaCl gradient, and the fractions containing toxin were pooled.

Cry3Aa was used as a negative control in binding studies. *B. thuringiensis* subsp. *tenebrionis* was cultured using CCY broth as for the other toxins. Crystalline inclusions were isolated by discontinuous sucrose density centrifugation (13) and then solubilized in 50 mM $NaHCO_3$ (pH 10.5) with 1 mM dithiothreitol (1 h at 37°C). Following centrifugation (27,000 × *g*, 30 min), the protoxin was activated with a 50% slurry of immobilized trypsin (Pierce) for 30 min at 37°C with shaking.

Toxin affinity for CAD3 was measured using the method of Friguet et al. (24). Various concentrations of Cry1Aa13, CryMK.123 and Cry3Aa (0.1 to 2,000 nM) were mixed with a constant amount of CAD3 (4 nM) in BPBS-T and allowed to reach equilibrium (15 h, 4°C). Meanwhile, an ELISA plate was coated with 10 μg/ml Cry1Aa13 in PBS (15-h incubation at 4°C), washed three times with PBS-T, blocked for 30 min with BPBS-T, and then washed three more times with PBS-T. A portion of each toxin/CAD3 mixture was transferred to the ELISA plate and incubated for 1 h at room temperature. Bound CAD3 was detected as described earlier in this section.

TABLE 1. Percentages of correctly assembled Crybody library variants, as determined by sequence analysis

Library	No. of variants	% of correctly assembled Crybody library variants				
		5′ junction[a]	CDR-H3 insert[b]	3′ junction[c]	Framework[d]	Assembly[e]
cc1	9	100	89	100	67	67
cc2	10	100	100	100	90	90
cc3	9	100	89	100	100	89
cc12	12	100	92	100	67	58
cc13	11	100	91	100	73	73
cc23	12	100	92	100	67	67
cc123	10	100	90	90	80	60
Total	73	100	92	99	77	71

[a] The sequence was GGT at the junction.
[b] The length of the insert was evenly divisible by 3.
[c] The sequence was TGG or TGC at the junction.
[d] Sixty base pairs of sequence upstream or downstream of the insertion were free of point mutations, insertions, and deletions.
[e] The assembly was error free over the entire sequence.

RESULTS

Library assembly and analysis. In order to investigate fully the suitability of the domain II apical loops for replacement, seven different libraries were constructed by combining the framework of Cry1Aa13 with CDR-H3 sequences obtained from a human antibody library. Each Crybody library was created by replacing the apical loops of Cry1Aa13 domain II, as defined by the X-ray crystal structure (30), with CDR-H3 sequences at a single site (cc1, cc2, and cc3), two sites (cc12, cc13, and cc23), or at all three sites (cc123), as shown in Fig. 2a and b. The assembly of each library was carried out in three steps, using a method adapted from that reported by Zeytun et al. (85). As detailed in Fig. 2c, this involved the recovery of CDR-H3 sequences from a high diversity phage display antibody library, amplification of framework regions from the *cry1Aa13* gene, and overlap extension PCR to join the CDR-H3 sequences to the Cry toxin framework. Cassettes for each of the seven libraries were then inserted into a *B. thuringiensis* expression vector (pCP0) encoding the remainder of the Cry1Aa13 protoxin.

The success of assembly was measured by sequencing a selection of Crybody cassettes from each library (see the supplemental material for sequence details). In total, 73 variants were selected at random, and all were unique (Table 1). In all the cassettes sequenced, the 5′ junction of the framework and the CDR-H3 insert was found to be error free. A high success rate was also achieved at the 3′ junction, where only 1 of 128

FIG. 2. Crybody libraries and their construction. (a) Schematic representation of the seven Crybody libraries derived from *cry1Aa13* and a human scFv antibody library. Sequences encoding loop 1, loop 2, and loop 3 of *cry1Aa13* are shown in blue, green, and yellow, respectively. CDR-H3 sequences are shown in red. The three domains encoded by *cry1Aa13* are labeled I, II, and III. V_L and V_H indicate the antibody domains. (b) Sequences of Crybodies with CDR-H3 insertions at site 1, 2, or 3. Adaptor codons are shown in bold, and the general CDR-H3 sequence is in red. The block arrows show secondary structure as defined by Grochulski et al. (30). (c) Overview of the three-step assembly strategy used to construct the cc123 library, involving (1) the recovery of CDR-H3 sequences from the scFv antibody library and their ligation to synthetic double-stranded DNA adaptor molecules corresponding to sequences adjacent to *cry1Aa13* domain II loops, (2) PCR amplification of *cry1Aa13* sequences encoding the toxin framework adjacent to the domain II loops, and (3) a series of overlap extension PCRs to join the recovered CDR-H3 sequences and the toxin framework sequences. Primers, restriction sites, and DNA fragments relevant to the assembly are labeled.

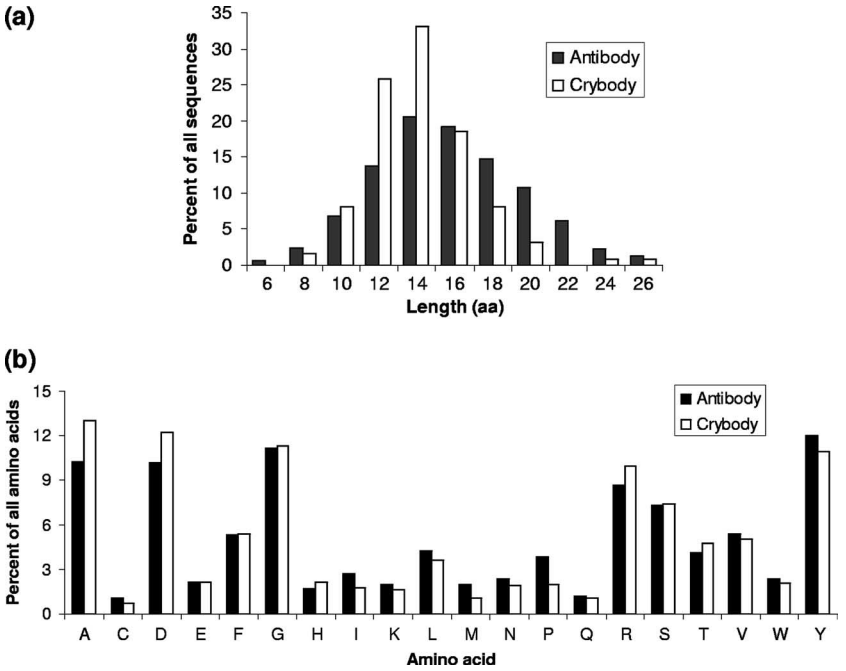

FIG. 3. Comparison of the lengths (a) and amino acid compositions (b) of Crybody-derived CDR-H3 sequences to those of antibody CDR-H3 sequences from a large database (84).

junctions was assembled incorrectly. In 92% of all the library cassettes, the length of the CDR-H3 insert was a multiple of 3, as would be expected if a genuine CDR-H3 sequence was present. When this was not the case, a single base pair deletion was detected, resulting in a frameshift mutation. Overall, errors were most frequently encountered in the toxin framework sequence, and most (19/21) occurred within the 60-bp toxin adaptor sequences flanking either side of the CDR-H3 sequence. These errors included insertions, deletions, and point mutations. Libraries modified at a single loop had a higher proportion of correctly assembled cassettes than those with multiple loop modifications.

Having obtained a high proportion of correctly assembled Crybody cassettes in each library, it was essential to determine whether the inserts were genuine CDR-H3 sequences and, if so, whether they were representative of the original library's CDR-H3 population. Since information on the CDR-H3 sequences present in the phage display antibody library was not available, a translation of the Crybody insert sequences was compared to a large collection of human antibody CDR-H3 sequences compiled by Zemlin et al. (84). This database contained 4,471 unique, functional CDR-H3 sequences derived from the Kabat (36) and IMGT (46) databases as of October 2002. As shown in Fig. 3a, the lengths of 124 Crybody-derived CDR-H3 sequences were compared to the lengths of 4,751 antibody-derived sequences. The mean length of the Crybody-derived CDR-H3 sequences was 13.6 ± 2.8, compared to 15.2 ± 4.1 for sequences obtained from the Zemlin database. While the average mean lengths were similar, the Crybody-derived CDR-H3 sequences were significantly shorter ($t = 4.24$, 4,873 degrees of freedom, $P = 2 \times 10^{-5}$, two-tailed distribution). The range of CDR-H3 lengths from Crybodies was 7 to 25, compared to 1 to 34 for sequences obtained from the Zemlin database. This did not necessarily indicate that Crybody CDR-H3 lengths were more constrained, as the sample size of the Zemlin database was considerably larger and would be expected to have more extreme variants. The overall amino acid composition of the two populations was also compared (Fig. 3b) and differed significantly ($\chi^2 = 64$, 19 degrees of freedom, $P = 1.0 \times 10^{-6}$); however, when the frequencies of individual amino acid residues were compared, only the usage of alanine and proline differed significantly between the two populations ($\chi^2 = 12$ to 15, $P < 0.05$, second level χ^2 test [14]). Thus, despite some minor differences, the results suggested that overall the two sets of CDR-H3 sequences had similar characteristics and that the process of assembling the Crybody libraries did not substantially bias the natural distribution of CDR-H3 length or amino acid composition.

Crystal formation. To investigate the effect of CDR-H3 loop replacement on toxin stability, Crybodies with uninterrupted open reading frames were expressed in sporulating *B. thuringiensis* IPS 78/11 to induce the production of crystalline inclusions. Table 2 shows that crystal production varied widely among the different libraries. In libraries with CDR-H3 insertions at a single site (cc1, cc2, and cc3), the proportion of constructs producing crystals was high. Crystal production varied from 78 to 89% among the three libraries. When only correctly assembled constructs were considered, this proportion increased to 83 to 100%. In libraries containing CDR-H3 insertions at two sites, crystal production was less consistent. Of the correctly assembled cc12 Crybodies, 71% were observed to produce crystals. Fewer cc23 constructs formed crystals (5/8 of correctly assembled clones), and none of the cc13 Crybodies formed crystals. When CDR-H3 sequences were introduced at all three sites (cc123), none of the constructs were found to produce Crybody crystals.

TABLE 2. Numbers and percentages of Crybody constructs in each library that produced crystalline inclusions when expressed in sporulating *B. thuringiensis* IPS 78/11

Library	All constructs		Constructs with uninterrupted open reading frames		Correctly assembled constructs	
	No./total	%	No./total	%	No./total	%
cc1	7/9	78	7/8	88	5/6	83
cc2	8/10	80	8/9	89	8/9	89
cc3	8/9	89	8/8	100	8/8	100
cc12	7/12	58	7/10	70	5/7	71
cc13	0/11	0	0/9	0	0/7	0
cc23	5/12	42	5/8	63	5/8	63
cc123	0/10	0	0/7	0	0/6	0
Total	35/73	48	35/59	59	31/51	61

To gain a better understanding of the factors influencing the production of crystalline inclusions, the theoretical chemical properties of Crybody CDR-H3 sequences were examined. First, variation in the levels of CDR-H3 hydropathy (43) was considered. The average level of hydropathy of each CDR-H3 insert (including adaptor codons) was calculated by summing the level of hydropathy of each residue in the sequence and dividing by the total number of residues. By this method, positive values corresponded to the sequences with an overall hydrophobic character and negative values to the sequences with a hydrophilic character. When all Crybody constructs were considered, the mean hydropathy value of the insert sequences was −0.52 (range, −1.65 to 0.89), and thus, the majority of the sequences were hydrophilic. By comparison, the average level of hydropathy of the natural toxin loops was −1.33 (loop 1), −1.03 (loop 2), and 0.32 (loop 3). Figure 4a shows the average levels of hydropathy of the CDR-H3 inserts from all Crybody constructs with uninterrupted open reading frames.

To test whether the average insert level of hydropathy could account for the differences in the success of crystal production observed among the different Crybody libraries, analysis of variance (ANOVA) was used. First, the average levels of hydropathy of the individual CDR-H3 sequences in each construct were averaged according to library, and the variance was determined. When these parameters were compared, no statistical difference was found ($F[6,78] = 0.44$, $P = 0.85$), as would be expected if the library construction was unbiased. Next, it was of interest to determine whether the combined average level of hydropathy of the domain II loops had an effect on crystal production. This value was calculated by summing the levels of hydropathy of all the domain II loop residues and dividing the result by the total number of residues (Fig. 4b). Depending on the library, this value was based solely on CDR-H3 sequences or a combination of CDR-H3 and natural toxin loop sequences. The differences in the mean combined average levels of hydropathy were found to be statistically significant ($F[6,44] = 6.08$, $P = 0.0001$). Using Scheffé post hoc analysis, differences were found between cc2 and cc3 ($F = 4.23$, $P < 0.01$) and between cc3 and cc12 ($F = 3.27$, $P < 0.01$), but there was no correlation between the mean combined average

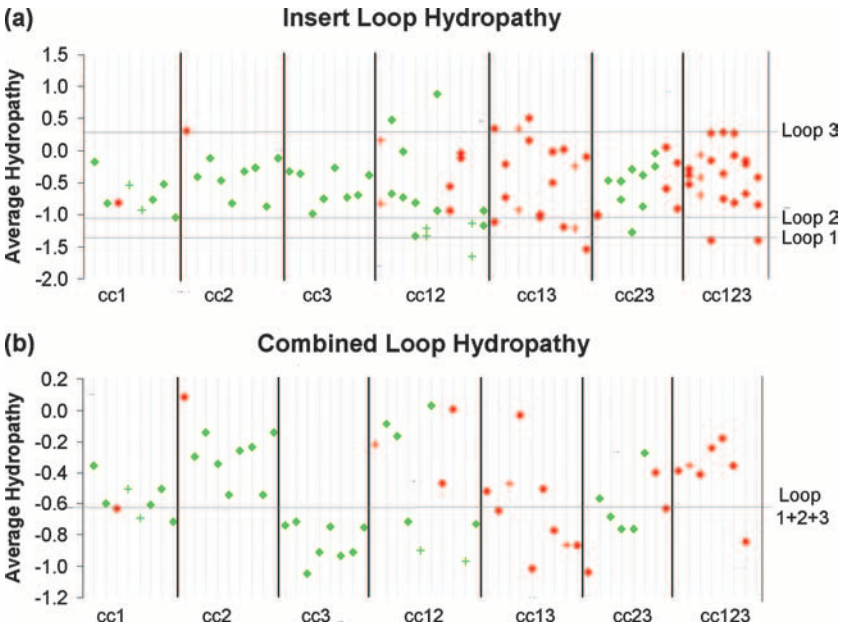

FIG. 4. The average levels of hydropathy of (a) individual CDR-H3 sequences or (b) the combination of CDR-H3 sequences and natural toxin loops found in Crybodies with uninterrupted open reading frames. Crybodies that formed or failed to form crystalline inclusions when expressed in sporulating *B. thuringiensis* IPS 78/11 are shown in green and red, respectively. Correctly assembled Crybodies or those with framework mutations are represented by diamonds and plus signs, respectively. The average levels of hydropathy of the natural toxin loops are labeled and shown by gray horizontal lines. From left to right, the identity of each construct is as follows: for the cc1 library, 8, 11, 13, 14, 15, 16, 21, and 25; for the cc2 library, 2, 4, 5, 6, 9, 20, 22, 26, and 30; for the cc3 library, 2, 6, 9, 10, 16, 17, 20, and 24; for the cc12 library, 4, 11, 12, 13, 15, 17, 24, 25, 26, and 28; for the cc13 library, 3, 4, 9, 11, 12, 15, 16, 20, and 22; for the cc23 library, 1, 2, 3, 8, 14, 21, 23, and 24; and for the cc123 library, 1, 2, 5, 7, 8, 9, and 10.

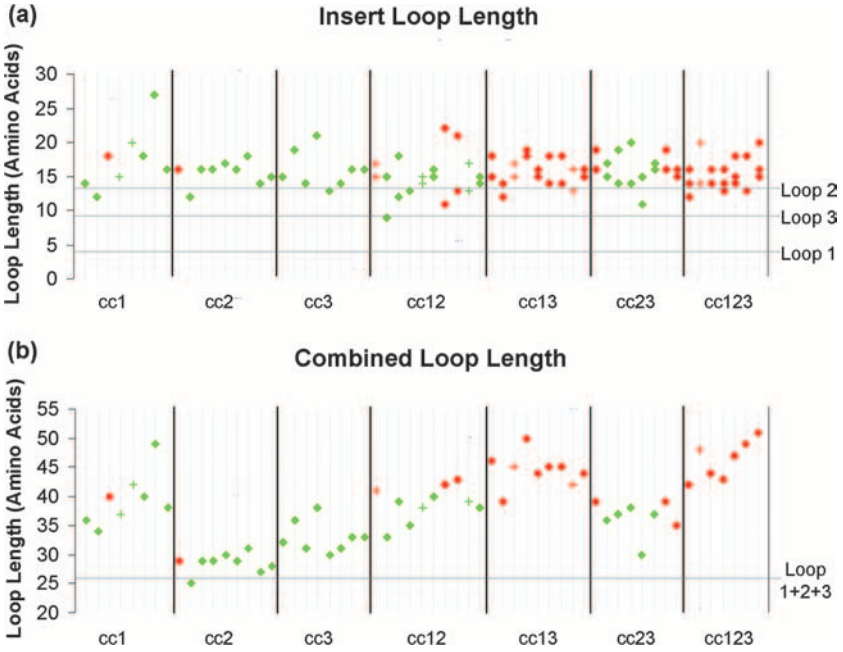

FIG. 5. The length of (a) individual CDR-H3 sequences or (b) the combination of CDR-H3 sequences and natural toxin loops found in Crybodies with uninterrupted open reading frames that formed (green) or failed to form (red) crystalline inclusion when expressed in sporulating *B. thuringiensis* IPS 78/11. Correctly assembled Crybodies are represented by diamonds, whereas Crybodies with framework mutations are shown by plus signs. The lengths of the natural toxin loops are labeled and shown by gray horizontal lines. The identity of each construct is as reported in the legend to Fig. 4.

level of hydropathy and the percentage of crystal formation using Pearson's r ($r = 0.15$, 6 degrees of freedom, $P > 0.01$). Overall, these results suggested that variation in the average levels of hydropathy of the CDR-H3 sequences, regardless of the site of the loop substitution or the number of loops substituted, could not account for differences in the success of crystal production among the libraries and thus could not be used to explain why crystal production failed in the cc13 and cc123 libraries.

CDR-H3 sequences vary widely in their lengths, and thus, it was of interest to determine whether certain lengths were more or less likely to be found in the Crybodies that formed crystalline inclusions. Figure 5a shows the lengths of the CDR-H3 sequences (including adaptor amino acids) found in constructs from each Crybody library. When the mean CDR-H3 lengths of the libraries were compared by ANOVA, no statistical difference was found ($F[6,78] = 0.84$, $P = 0.54$), and thus, individual loop length per se could not be used to explain why the cc13 and cc123 library constructs failed to form crystals.

Next, we examined whether the combined length of the domain II loops had an effect on the success of crystal production. As shown in Fig. 5b, all but one of the Crybodies with uninterrupted reading frames had a combined loop length greater than the naturally occurring length of 26 amino acids. Among the libraries, the differences in the mean combined loop lengths were found to be significant by ANOVA ($F[6,44] = 26$, $P < 0.00001$), and by Scheffé post hoc analysis ($\alpha = 0.01$), libraries were classified into three overlapping groups. The cc2 and cc3 libraries had the shortest average loop lengths and formed the first group. Library cc3 was also part of the intermediate group, along with cc23, cc12, and cc1. The last group consisted of libraries with the longest average combined loop lengths and included cc1, cc12, cc13, and cc123. Pearson's r was used to test the correlation between the average combined loop length and the percentage of constructs forming crystals; a significant negative correlation was found ($r = -0.85$, 6 degrees of freedom, $P = 0.02$). These results indicated that the combined loop length per se may be an important determinant of crystal production success and suggested a possible reason why none of the cc13 or cc123 Crybody constructs formed crystalline inclusions.

Toxin solubilization and activation. Crybody constructs that formed crystalline inclusions were further tested for their ability to solubilize under standard in vitro conditions. Cry1Aa13 and the non-crystal-producing construct cc2.2 were used as positive and negative controls, respectively. As shown in Fig. 6, several bands were detected in the solubilized Cry1Aa13 sample. The most intensely stained band ran above the 116-kDa marker and was the expected size of the full-length protoxin (a theoretical molecular mass of 133 kDa); the lower bands were probably partially digested protoxin products. Only faint bands were detected in the no-crystal control. All crystal-forming Crybodies were found to undergo solubilization, and the majority had a banding pattern similar to that of the wild-type toxin. Notable exceptions were cc1.16, cc1.21, cc12.12, cc12.28, and cc23.8, where the detection of full-length protoxin was negligible.

Crybody resistance to proteolysis was tested by incubation with trypsin. As shown in Fig. 6, trypsin-treated Cry1Aa13 was detected as a single major band near the expected apparent molecular mass of 58 kDa (56). A minor band detected below the 24-kDa marker was present in all samples and migrated at

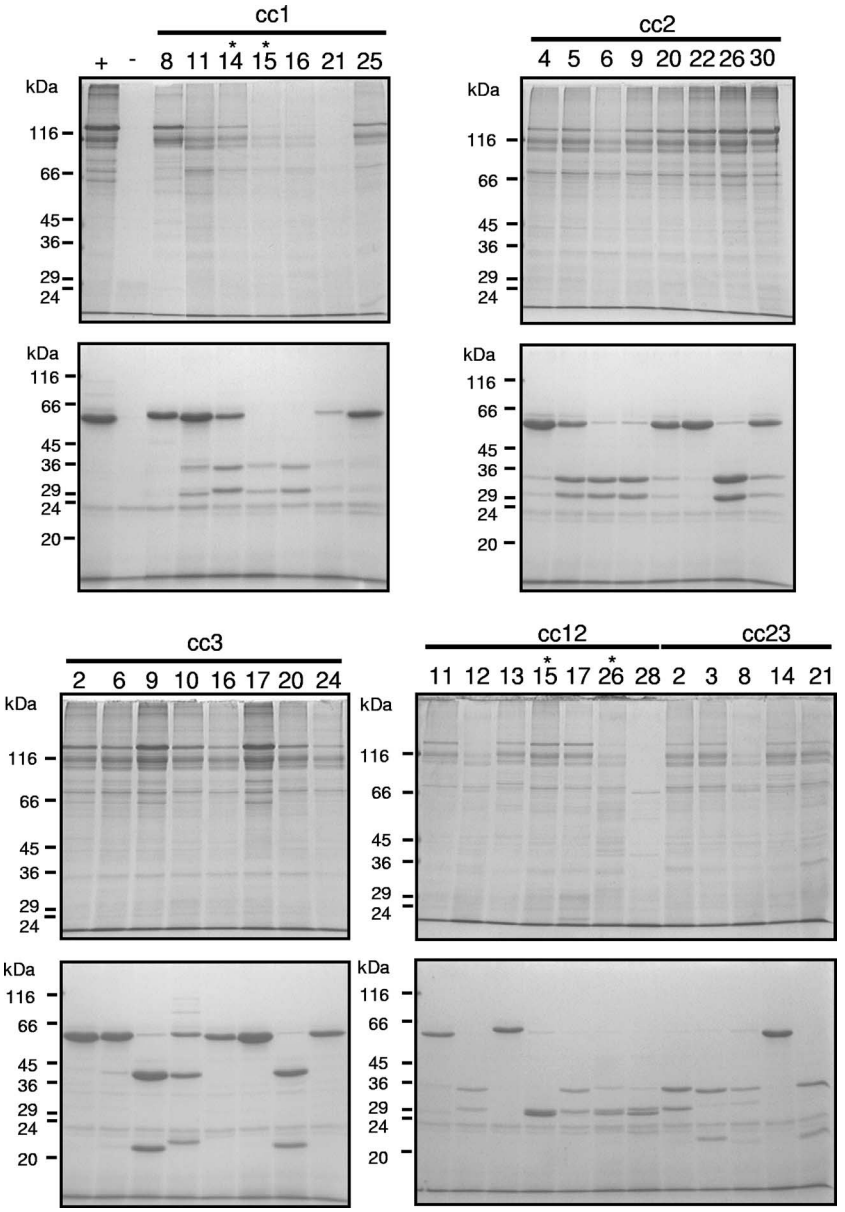

FIG. 6. Coomassie blue-stained SDS-PAGE gels showing solubilized (upper gels) or trypsin-treated (lower gels) Crybodies expressed in sporulating *B. thuringiensis* IPS 78/11. + and − indicate lanes containing Cry1Aa13 or cc2.2 (crystal-negative control), respectively. Constructs with framework mutations are indicated by an asterisk.

the expected molecular mass of trypsin. Crybodies treated with trypsin generally underwent internal cleavage, and the size of the products suggested cleavage within the CDR-H3 loop or loops. This was confirmed in construct cc2.26 by N-terminal sequencing. The upper cleavage product had the sequence IETGY, corresponding to the start of the active toxin domain. The lower cleavage product had the sequence TFDP, indicating cleavage after an arginine in the CDR-H3 loop.

Trypsin cleaves polypeptides at arginine and lysine residues, and thus, it was of interest to determine how the presence of these amino acids affected the extent of the internal cleavage. The total number of arginine and lysine residues in the CDR-H3 sequence of each Crybody was determined. Crybodies were classified as trypsin resistant, if no or only minor cleavage products were detected by SDS-PAGE analysis, or as trypsin susceptible. Resistant Crybodies included cc1.8, cc1.25, cc2.4, cc2.20, cc2.22, cc3.2, cc3.6, cc3.16, cc3.17, cc3.24, cc12.11, cc12.13, and cc23.14, as shown in Fig. 6. Next, Crybodies were grouped by the number of arginine or lysine residues in their CDR-H3 sequence and the percentage of resistant constructs determined. As shown in Fig. 7, Crybodies with fewer arginine or lysine residues in their CDR-H3 sequences were more frequently trypsin resistant; no internal cleavage was evident in those lacking these residues.

Toxicity. Toxicity toward *Manduca sexta* neonates was assessed at a single concentration using unpurified Crybodies in

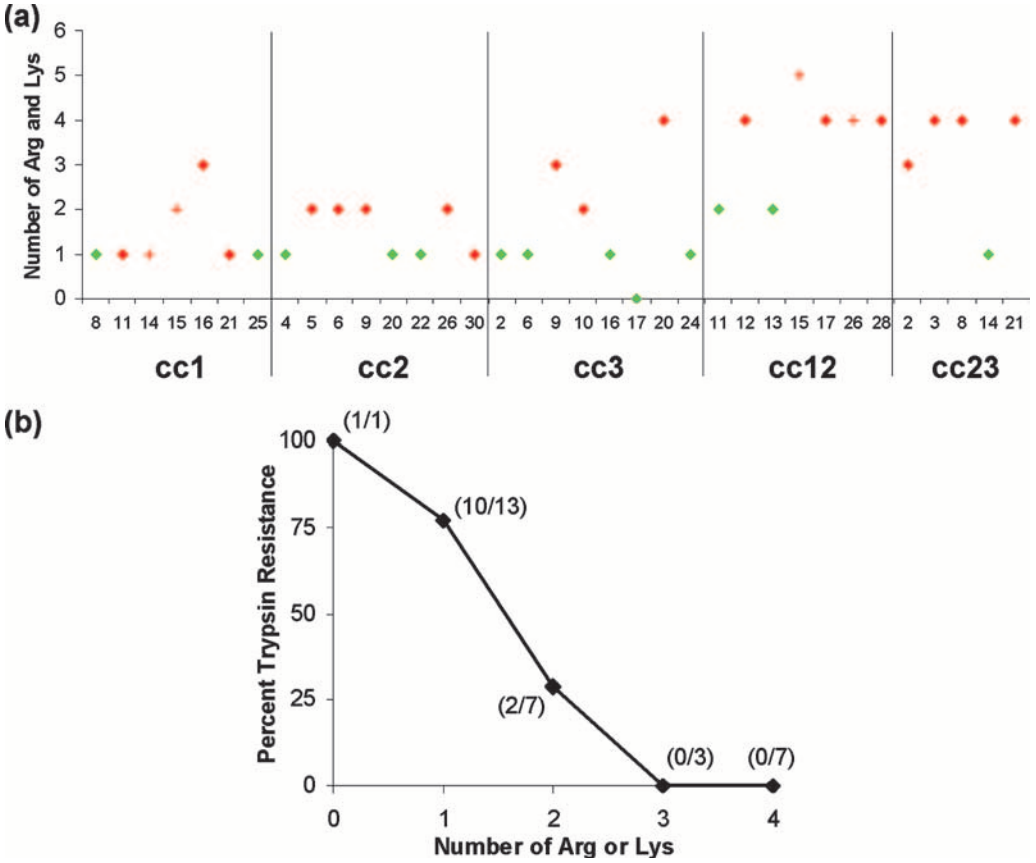

FIG. 7. The relationship between the presence of arginine or lysine residues in CDR-H3 inserts and Crybody sensitivity to internal trypsin cleavage. (a) The number of arginine or lysine residues present in CDR-H3 inserts of Crybodies susceptible (red) or resistant (green) to internal trypsin cleavage. Correctly assembled Crybodies are represented by diamonds, whereas Crybodies with framework mutations are shown by plus signs. (b) The percentages of Crybodies resistant to internal trypsin cleavage, grouped by the number of arginine or lysine residues present in their CDR-H3 sequence. The ratio of resistant to total Crybodies is shown in parentheses at each data point. Only correctly assembled Crybodies were considered in this analysis.

cultures of sporulated *B. thuringiensis* IPS 78/11 to determine how the replacement of natural loops with CDR-H3 sequences influenced toxin potency. By this method, distinct differences were evident among the different libraries (Fig. 8). In the cc1 library, all Crybodies showed at least some toxicity toward the larvae, although the level of toxicity was variable. Crybodies cc1.11 and cc1.25 showed the highest activity and killed all neonates in every trial, whereas clone cc1.8 killed only 17% of

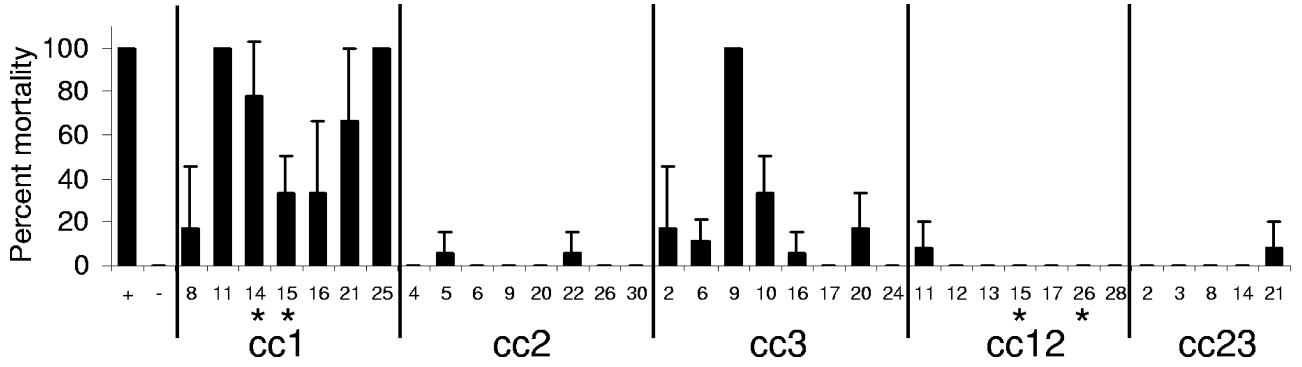

FIG. 8. Crybody toxicity toward *M. sexta* neonates. Strains of *B. thuringiensis* IPS 78/11 expressing wild-type Cry1Aa13 (+) or a Crybody (as indicated) were cultured in CCY medium supplemented with 6 μg/ml chloramphenicol until complete sporulation was observed by phase contrast microscopy (48 to 72 h). Twenty microliters of each culture was applied to the surface of *M. sexta* diet in 48-well plates. Control wells (−) contained only diet. Neonates were added and plates incubated for 5 days, at which point mortality was assessed. Crybodies from libraries cc1, cc2, and cc3 were tested in three independent trials, six insects per trial. Crybodies from libraries cc12 and cc23 were tested twice, six insects per trial. Asterisks indicate Crybodies with framework mutations.

the neonates on average. All Crybodies of the cc2 library, in contrast, showed negligible toxicity. Compared to the Crybodies of cc1, the cc3 Crybodies showed less toxicity overall, but clone cc3.9 showed maximal activity. The remaining cc3 Crybodies showed reduced activity, and all killed less than 35% of the neonates in the average trial. None of the clones in the cc12 and cc23 libraries showed significant activity toward any of the larvae. As the distribution of CDR-H3 lengths and levels of hydropathy was similar among all the libraries (Fig. 4 and Fig. 5), it seemed that the site of the CDR-H3 insertion was the most important factor in determining insect toxicity. Loop 2 seemed to be a particularly important determinant given that all libraries with CDR-H3 insertions at this site, regardless of the level of CDR-H3 hydropathy or length, showed negligible toxicity.

Binding specificity. Crybodies solubilized from partially purified spore/crystal mixtures were tested for their ability to bind to a segment of the *H. virescens* cadherin-like protein (HevCaLP) to determine how loop modification affected binding to natural receptors. This was carried out by ELISA using *E. coli*-expressed CAD3, a truncated form of HevCaLP containing the toxin binding region, and M1429$^-$, a version of CAD3 with a phenylalanine to aspartic acid mutation that abrogates Cry1Ab and Cry1Ac binding (82). As shown in Fig. 9a, Cry1Aa13 bound strongly to CAD3 but showed minimal binding to M1429$^-$, as expected. Surprisingly, all crystal-forming Crybodies bound strongly to CAD3, despite considerable differences in the amino acid sequence of the domain II loops. Since Crybody binding to M1429$^-$ was minimal, it appeared that the interaction between Crybodies and CAD3 was specific.

Crybody binding was also tested using purified toxin and receptors isolated from the midgut of *M. sexta*. The toxin Cry1Aa13.2.4D5 was selected for this purpose because its loop 2 CDR-H3 substitution, ^{368}RIILGSGPNNQEL^{380} to WGGD GFYAMDV, eliminates toxicity toward *M. sexta* neonates without affecting crystal formation or protease sensitivity (data not shown). Receptor binding was tested using the ligand blot technique, where BBMV were resolved by SDS-PAGE, transferred to a membrane, and then probed with solubilized, activated toxin. Like the wild-type toxin, Cry1Aa13.2.4D5 detected a 210-kDa band corresponding to the *M. sexta* cadherin-like protein Bt-R_1 (74) (Fig. 9b).

Analysis of a Cry1Aa13 derivate with mutations at all three loops. Because all Crybodies bound to CAD3 despite modifications to their domain II apical loops, the importance of this region in cadherin binding was unclear. Crybodies with loop substitutions at one or two sites retained binding specificity, indicating that none of the natural toxin loops were essential for receptor binding; however, it was not possible to test the effect of loop substitution at all three sites simultaneously since none of the cc123 Crybodies formed crystals. To address this problem, a Cry1Aa13 mutant with modifications at all three loops was created. At loop 1, the sequence ^{310}HRGF^{313} was changed to HSGF. Loop 2 was deleted by replacing ^{367}RRII LGSGPNNQE^{379} with the sequence RGGE. Loop 3 was modified by replacing the sequence ^{438}SQAAGAVYT^{446} with SSGST. The expression of this Cry1Aa13 derivate, called CryMK.123, was carried out in sporulating *B. thuringiensis* IPS 78/11, and crystals with wild-type morphology were observed. Using standard in vitro conditions, these crystals could be solubilized, and trypsin treatment yielded toxin of the expected molecular weight with no evidence of internal cleavage (data not shown). Consistent with other loop 2 mutants tested in this study, CryMK.123 was not toxic to *M. sexta* at the highest toxin concentration tested (2 $\mu g/cm^2$; data not shown).

To determine whether CryMK.123 could bind to CAD3, a competitive ELISA was carried out. Various concentrations of purified, activated Cry1Aa13, Cry3Aa, or CryMK.123 were incubated with a constant concentration of CAD3 in solution and allowed to reach equilibrium. A portion of each sample was then transferred to an ELISA plate coated with Cry1Aa13 to measure the amount of unbound CAD3 remaining in solution. As shown in Fig. 9c, increasing concentrations of Cry1Aa13 and CryMK.123, but not the negative control toxin Cry3Aa, decreased the amount of free CAD3 in solution. The dissociation constants (K_d) for the interactions between Cry1Aa13 or CryMK.123 and CAD3 were determined using the method described by Friguet et al. (24) and were found to be 220 nM (95% confidence interval, 200 to 240 nM) and 576 nM (95% confidence interval, 515 to 638 nM), respectively. Thus, even when all three apical loops of domain II were modified or deleted, the binding affinity for CAD3 decreased by only 2.6-fold.

DISCUSSION

Combinatorial molecular biology is an effective method to generate proteins with novel binding specificities. The process is carried out naturally in jawed vertebrates, in which multiple immunoglobulin gene segments recombine during B-cell maturation to form innumerable sequence combinations leading to antibodies with diverse binding specificities. These recombined antibody genes have been used to create large phage display libraries from which antibodies for diagnostic and therapeutic purposes have been derived (75).

In this study, we sought to utilize the diversity of existing antibody CDR-H3 sequences to generate Cry toxins with novel properties. The method employed to create Crybodies proved to be highly successful; the majority of the variants were found to be error free over the entire sequence, and the length distribution and amino acid composition of the CDR-H3 inserts were comparable to those found in natural antibodies. These results suggest that the assembly method developed in this study could be used to generate Crybody libraries suitable for selection or screening. The common domain structure of the main family of Cry toxins and their similar mode of action suggest that diversity may be introduced into any such toxin using a similar method.

Analysis of the Crybody libraries revealed marked differences in crystal production. The highest proportions of constructs forming crystals were found in the single-loop substitution libraries cc1, cc2, and cc3. That most CDR-H3 insertions were well tolerated at loop 1 was particularly remarkable given the large difference in length between the natural toxin loop (4 amino acids) and the median CDR-H3 insert (15 amino acids, including adaptor codons). That all three library constructs could tolerate CDR-H3 substitutions with variable lengths and hydropathy was an important result given the ultimate goal of generating Crybodies with diverse specificities.

While the high proportion of single-loop substitution librar-

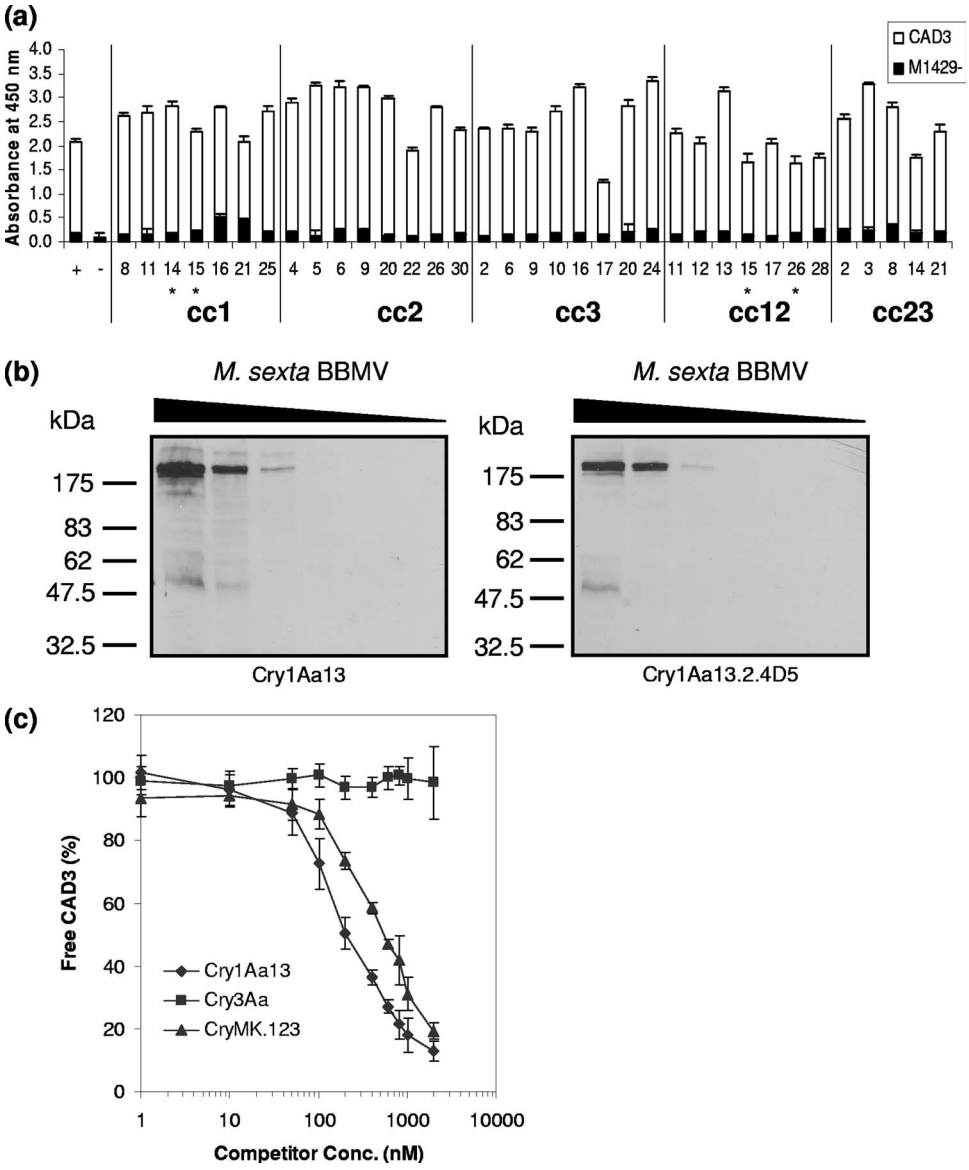

FIG. 9. Cry toxin receptor binding. (a) Crybody binding to the cadherin receptors CAD3 and M1429$^-$, as determined by ELISA. Solubilized Crybodies, Cry1Aa13 (+), and a control without toxin (−) were used to coat the wells of microtiter plates. Wells were probed with CAD3, M1429$^-$, or buffer alone and bound receptor detected with Ni-nitrilotriacetic acid horseradish peroxidase. Absorbance values were corrected by subtracting the absorbance of corresponding controls incubated without receptors. The means and standard deviations of the results from four replicates are shown. Asterisks indicate Crybodies with mutations in the toxin framework. (b) Analysis of Cry1Aa13 and Cry1Aa13.2.4D5 binding to *M. sexta* BBMV receptors by ligand blot assay. On duplicate gels, 230, 46, 9.2, 1.8, 0.37, or 0.070 μg of total BBMV protein was resolved by SDS-PAGE and then electrotransferred to nitrocellulose membranes. The blots were then blocked and probed with either activated Cry1Aa13 or Cry1Aa13.2.4D5. Toxin binding was detected by incubation with anti-Cry1Aa polyclonal antibodies followed by anti-rabbit IgG antibodies conjugated to horseradish peroxidase. (c) Analysis of Cry1Aa13, CryMK.123, and Cry3Aa binding to CAD3. Various concentrations of Cry1Aa13, CryMK.123, and Cry3Aa were mixed with a constant amount of CAD3 (4 nM) and allowed to reach equilibrium. A portion of each sample was then transferred to an ELISA plate previously coated with Cry1Aa13, and the amount of free CAD3 was detected as described for panel a. The means and standard deviations of the results from three independent experiments are shown.

ies that formed crystals indicated that none of the natural toxin loops was essential for crystal formation, considerable differences were observed among the multiple substitution libraries; the majority of the cc12 and cc23 constructs formed crystals, but none were formed by cc13 and cc123 constructs. A detailed analysis of the insert sequences was undertaken, and combined loop length was found to be an important determinant of Crybody stability. While not conclusive, these results suggested that a reduction in the average CDR-H3 length may permit the generation of crystal-forming cc13 and cc123 Crybodies. This hypothesis was supported by the finding that CryMK.123—a Cry1Aa13 derivative with substitutions at loop 1 and deletions at loops 2 and 3—formed crystals with wild-type morphology (data not shown).

Sensitivity to proteolytic degradation is a common method of testing whether mutations to Cry toxins cause global

changes in structure. Since Cry1Aa13 naturally contains 44 arginines and 2 lysines within its protease-resistant core, global changes in structure resulting from CDR-H3 substitutions should be easily identified by treatment with trypsin. Almost all Crybodies were found to undergo at least partial internal cleavage. The pattern of banding was relatively similar within libraries but differed among libraries, suggesting the introduction of CDR-H3-dependent trypsin cleavage sites rather than the exposure of existing arginine or lysine residues. This was supported by N-terminal sequencing results that showed the cleavage of cc2.26 after a CDR-H3 arginine and the apparent positive correlation between trypsin sensitivity and the number of CDR-H3 arginine or lysine residues present. This finding will benefit the design of future libraries, for which the choice of CDR-H3 sequences could be restricted to those lacking arginine or lysine residues.

Another major aim of Crybody analysis was to determine how the replacement of domain II loops with CDR-H3 sequences would affect the natural specificity of the toxin. To determine the effect of CDR-H3 replacement on toxicity, *M. sexta* neonates were fed cultures of sporulated *B. thuringiensis* IPS 78/11 expressing Crybody crystals. Considerable differences were observed among the different libraries. The highest degree of toxicity was observed with cc1 Crybodies. Given that two of the seven cc1 Crybodies tested killed all the neonates in every trial, it seemed unlikely that natural loop 1 plays a direct role in *M. sexta* toxicity. These results were consistent with a recent study showing that mutating residues ^{311}RG^{312} to YQDL did not have a statistically significant effect on Cry1Aa toxicity toward *M. sexta* larvae (49). The effect of replacing loop 2 with CDR-H3 sequences was more severe, and none of the Crybodies in the cc2, cc12, or cc23 libraries showed significant toxicity toward the neonates. This result was expected given that alanine substitution of residues 365 to 371 eliminated Cry1Aa toxicity toward the related lepidopteran *Bombyx mori* (50). Previous results have also shown that loop 3 is an important determinant of toxicity, since the deletion of residues 440 to 443 decreased toxicity to *B. mori* and *M. sexta* by 23- and more than 62-fold, respectively. Interestingly, most cc3 Crybodies showed at least some toxicity to *M. sexta* neonates, and cc3.9 killed all neonates in every trial. Together, these results suggest that only loop 2 is essential for *M. sexta* neonate toxicity.

Crybodies were also tested for their abilities to bind to a truncated form of the *H. virescens* cadherin-like protein HevCaLP. The importance of HevCaLP as a Cry1A receptor has been well established. Gahan et al. (25) showed that the disruption of *BtR-4* (the HevCaLP gene) was linked to high levels of recessive resistance to Cry1Ac and cross-resistance to Cry1Ab and Cry1Aa, and Jurat-Fuentes et al. (40) reported that a wild-type *BtR-4* allele was necessary for HevCaLP production and Cry1Aa binding to BBMV. The interaction between the HevCaLP fragment CAD3 and Cry1Ab/Cry1Ac was shown by peptide competition to involve loop 3 and possibly loop 2 of Cry1Ab (82). While the domain II loops of Cry1Aa have not been directly tested for their role in binding to HevCaLP, loop 2 and loop 3 have been implicated in binding to the related *M. sexta* receptor Bt-R_1 (29), and Cry1Ab and Cry1Ac compete with Cry1Aa for binding to *H. virescens* BBMV (44). Mutations to Cry1Aa loop 2 and loop 3 have also been shown to reduce binding to *B. mori* and *M. sexta* BBMV (50, 63), but their effect on binding to an isolated cadherin receptor has not been reported.

Crybody binding to CAD3 and M1429$^-$ was compared to Cry1Aa13 at a single concentration to determine whether major differences in affinity could be detected. Unexpectedly, all Crybodies bound strongly to CAD3. Binding appeared to be specific, as none of the Crybodies bound to the M1429$^-$ point mutant. It was particularly surprising that Crybodies simultaneously modified at loop 2 and loop 3 showed no obvious reduction in binding given their proposed role in binding to BT-R_1 and that loop 3 and possibly loop 2 are believed to be important for Cry1Ab/Cry1Ac binding to HevCaLP. The finding that all Crybodies bound to CAD3 was also unexpected considering their differing toxicities toward *M. sexta* neonates. While binding and toxicity were tested with different species, the cadherin receptors are 60% identical and 76% similar (using the PAM250 matrix) over the region of CAD3. If the loss of toxicity associated with loop 2 replacement was due to a major reduction in affinity for the cadherin receptor, this should have been detected in the binding assay; however, no correlation was observed. These results were consistent with the finding that the loop 2 Cry1Aa13.2.4D5 mutant was not toxic toward *M. sexta* neonates, and yet binding to *M. sexta* BT-R_1 was comparable to Cry1Aa13 in a ligand blot assay. In addition, CryMK.123, a Cry1Aa13 derivative with amino acid deletions or substitutions in all three apical loops, bound to CAD3 with an affinity only 2.6-fold lower than that of the wild-type toxin. Overall, these results provide no indication that the domain II loops of Cry1Aa are directly involved in cadherin binding.

Although the true cadherin binding site appears to be distinct from the domain II loops, the fact remains that modifications to the domain loops do influence toxicity. As such, it should be possible to improve the insecticidal properties of Crybodies through loop substitution regardless of the actual function of the domain II loops or the mechanism by which they influence toxicity. By eliminating CDR-H3 sequences with lysines and arginines and decreasing the average loop length, the utility of Crybody libraries may be further improved.

ACKNOWLEDGMENTS

We thank Trevor Sawyer for his expert technical assistance with this project.

The work of C.R.P. was supported financially by the Cambridge Commonwealth Trust, the Cambridge Philosophical Society, the C. T. Taylor Trust, the Beverly and Raymond Sackler Studentship Fund, the Canadian Centennial Scholarship Fund, the Alexander James Keith Fund, and Darwin College Cambridge. This work was also made possible by the generous support of Cambridge Antibody Technology and Syngenta.

REFERENCES

1. **Abdullah, M. A., O. Alzate, M. Mohammad, R. J. McNall, M. J. Adang, and D. H. Dean.** 2003. Introduction of *Culex* toxicity into *Bacillus thuringiensis* Cry4Ba by protein engineering. Appl. Environ. Microbiol. **69:**5343–5353.
2. **Abdullah, M. A., and D. H. Dean.** 2004. Enhancement of Cry19Aa mosquitocidal activity against *Aedes aegypti* by mutations in the putative loop regions of domain II. Appl. Environ. Microbiol. **70:**3769–3771.
3. **Bell, R. A., and F. G. Joachim.** 1976. Techniques for rearing laboratory colonies of tobacco hornworms and pink bollworms. Ann. Entomol. Soc. Am. **69:**365–373.
4. **Binz, H. K., P. Amstutz, and A. Pluckthun.** 2005. Engineering novel binding proteins from nonimmunoglobulin domains. Nat. Biotechnol. **23:**1257–1268.

5. **Binz, H. K., and A. Pluckthun.** 2005. Engineered proteins as specific binding reagents. Curr. Opin. Biotechnol. **16:**459–469.
6. **Bone, E. J., and D. J. Ellar.** 1989. Transformation of *Bacillus thuringiensis* by electroporation. FEMS Microbiol. Lett. **49:**171–177.
7. **Boonserm, P., P. Davis, D. J. Ellar, and J. Li.** 2005. Crystal structure of the mosquito-larvicidal toxin Cry4Ba and its biological implications. J. Mol. Biol. **348:**363–382.
8. **Boonserm, P., M. Mo, C. Angsuthanasombat, and J. Lescar.** 2006. Structure of the functional form of the mosquito larvicidal Cry4Aa toxin from *Bacillus thuringiensis* at a 2.8-angstrom resolution. J. Bacteriol. **188:**3391–3401.
9. **Bravo, A.** 1997. Phylogenetic relationships of *Bacillus thuringiensis* δ-endotoxin family proteins and their functional domains. J. Bacteriol. **179:**2793–2801.
10. **Bravo, A., I. Gómez, J. Conde, C. Muñoz-Garay, J. Sánchez, R. Miranda, M. Zhuang, S. S. Gill, and M. Soberón.** 2004. Oligomerization triggers binding of a *Bacillus thuringiensis* Cry1Ab pore-forming toxin to aminopeptidase N receptor leading to insertion into membrane microdomains. Biochim. Biophys. Acta **1667:**38–46.
11. **Burton, S. L., D. J. Ellar, J. Li, and D. J. Derbyshire.** 1999. *N*-acetylgalactosamine on the putative insect receptor aminopeptidase N is recognised by a site on the domain III lectin-like fold of a *Bacillus thuringiensis* insecticidal toxin. J. Mol. Biol. **287:**1011–1022.
12. **Carroll, J., and D. J. Ellar.** 1993. An analysis of *Bacillus thuringiensis* δ-endotoxin action on insect-midgut-membrane permeability using a light-scattering assay. Eur. J. Biochem. **214:**771–778.
13. **Carroll, J., J. Li, and D. J. Ellar.** 1989. Proteolytic processing of a coleopteran-specific δ-endotoxin produced by *Bacillus thuringiensis var. tenebrionis.* Biochem. J. **261:**99–105.
14. **Collis, A. V., A. P. Brouwer, and A. C. Martin.** 2003. Analysis of the antigen combining site: correlations between length and sequence composition of the hypervariable loops and the nature of the antigen. J. Mol. Biol. **325:**337–354.
15. **Crickmore, N., and D. J. Ellar.** 1992. Involvement of a possible chaperonin in the efficient expression of a cloned CryIIA δ-endotoxin gene in *Bacillus thuringiensis*. Mol. Microbiol. **6:**1533–1537.
16. **de Maagd, R. A., P. L. Bakker, L. Masson, M. J. Adang, S. Sangadala, W. Stiekema, and D. Bosch.** 1999. Domain III of the *Bacillus thuringiensis* δ-endotoxin Cry1Ac is involved in binding to *Manduca sexta* brush border membranes and to its purified aminopeptidase N. Mol. Microbiol. **31:**463–471.
17. **de Maagd, R. A., A. Bravo, and N. Crickmore.** 2001. How *Bacillus thuringiensis* has evolved specific toxins to colonize the insect world. Trends Genet. **17:**193–199.
18. **de Maagd, R. A., M. S. G. Kwa, H. van der Klei, T. Yamamoto, B. Schipper, J. M. Vlak, W. J. Stiekema, and D. Bosch.** 1996. Domain III substitution in *Bacillus thuringiensis* delta-endotoxin CryIA(b) results in superior toxicity for *Spodoptera exigua* and altered membrane protein recognition. Appl. Environ. Microbiol. **62:**1537–1543.
19. **de Maagd, R. A., M. Weemen-Hendriks, J. W. Molthoff, and S. Naimov.** 2003. Activity of wild-type and hybrid *Bacillus thuringiensis* delta-endotoxins against *Agrotis ipsilon*. Arch. Microbiol. **179:**363–367.
20. **de Maagd, R. A., M. Weemen-Hendriks, W. Stiekema, and D. Bosch.** 2000. *Bacillus thuringiensis* delta-endotoxin Cry1C domain III can function as a specificity determinant for *Spodoptera exigua* in different, but not all, Cry1-Cry1C hybrids. Appl. Environ. Microbiol. **66:**1559–1563.
21. **Derbyshire, D. J., D. J. Ellar, and J. Li.** 2001. Crystallization of the *Bacillus thuringiensis* toxin Cry1Ac and its complex with the receptor ligand *N*-acetyl-D-galactosamine. Acta Crystallogr. D **57:**1938–1944.
22. **Dorsch, J. A., M. Candas, N. B. Griko, W. S. Maaty, E. G. Midboe, R. K. Vadlamudi, and L. A. Bulla, Jr.** 2002. Cry1A toxins of *Bacillus thuringiensis* bind specifically to a region adjacent to the membrane-proximal extracellular domain of BT-R(1) in *Manduca sexta*: involvement of a cadherin in the entomopathogenicity of *Bacillus thuringiensis*. Insect Biochem. Mol. Biol. **32:**1025–1036.
23. **Flannagan, R. D., C. G. Yu, J. P. Mathis, T. E. Meyer, X. Shi, H. A. Siqueira, and B. D. Siegfried.** 2005. Identification, cloning and expression of a Cry1Ab cadherin receptor from European corn borer, Ostrinia nubilalis (Hübner) (Lepidoptera: Crambidae). Insect Biochem. Mol. Biol. **35:**33–40.
24. **Friguet, B., A. F. Chaffotte, L. Djavadi-Ohaniance, and M. E. Goldberg.** 1985. Measurements of the true affinity constant in solution of antigen-antibody complexes by enzyme-linked immunosorbent assay. J. Immunol. Methods **77:**305–319.
25. **Gahan, L. J., F. Gould, and D. G. Heckel.** 2001. Identification of a gene associated with Bt resistance in *Heliothis virescens*. Science **293:**857–860.
26. **Galitsky, N., V. Cody, A. Wojtczak, D. Ghosh, J. R. Luft, W. Pangborn, and L. English.** 2001. Structure of the insecticidal bacterial δ-endotoxin Cry3Bb1 of *Bacillus thuringiensis*. Acta Crystallogr. D **57:**1101–1109.
27. **Garcia-Robles, I., J. Sánchez, A. Gruppe, A. C. Martinez-Ramirez, C. Rausell, M. D. Real, and A. Bravo.** 2001. Mode of action of *Bacillus thuringiensis* PS86Q3 strain in hymenopteran forest pests. Insect Biochem. Mol. Biol. **31:**849–856.
28. **Gilliland, A., C. E. Chambers, E. J. Bone, and D. J. Ellar.** 2002. Role of *Bacillus thuringiensis* Cry1 δ endotoxin binding in determining potency during lepidopteran larval development. Appl. Environ. Microbiol. **68:**1509–1515.
29. **Gómez, I., J. Miranda-Rios, E. Rudiño-Piñera, D. I. Oltean, S. S. Gill, A. Bravo, and M. Soberón.** 2002. Hydropathic complementarity determines interaction of epitope ^{869}HITDTNNK^{876} in *Manduca sexta* Bt-R_1 receptor with loop 2 of domain II of *Bacillus thuringiensis* Cry1A toxins. J. Biol. Chem. **277:**30137–30143.
30. **Grochulski, P., L. Masson, S. Borisova, M. Pusztai-Carey, J. L. Schwartz, R. Brousseau, and M. Cygler.** 1995. *Bacillus thuringiensis* CryIA(a) insecticidal toxin: crystal structure and channel formation. J. Mol. Biol. **254:**447–464.
31. **Höfte, H., and H. R. Whiteley.** 1989. Insecticidal crystal proteins of *Bacillus thuringiensis*. Microbiol. Rev. **53:**242–255.
32. **Hosse, R. J., A. Rothe, and B. E. Power.** 2006. A new generation of protein display scaffolds for molecular recognition. Protein Sci. **15:**14–27.
33. **Hua, G., J. L. Jurat-Fuentes, and M. J. Adang.** 2004. Fluorescent-based assays establish *Manduca sexta* Bt-R_{1a} cadherin as a receptor for multiple *Bacillus thuringiensis* Cry1A toxins in *Drosophila* S2 cells. Insect Biochem. Mol. Biol. **34:**193–202.
34. **Jenkins, J. L., M. K. Lee, S. Sangadala, M. J. Adang, and D. H. Dean.** 1999. Binding of *Bacillus thuringiensis* Cry1Ac toxin to *Manduca sexta* aminopeptidase-N receptor is not directly related to toxicity. FEBS Lett. **462:**373–376.
35. **Jenkins, J. L., M. K. Lee, A. P. Valaitis, A. Curtiss, and D. H. Dean.** 2000. Bivalent sequential binding model of a *Bacillus thuringiensis* toxin to gypsy moth aminopeptidase N receptor. J. Biol. Chem. **275:**14423–14431.
36. **Johnson, G., and T. T. Wu.** 2001. Kabat Database and its applications: future directions. Nucleic Acids Res. **29:**205–206.
37. **Jones, P. T., P. H. Dear, J. Foote, M. S. Neuberger, and G. Winter.** 1986. Replacing the complementarity-determining regions in a human antibody with those from a mouse. Nature **321:**522–525.
38. **Jurat-Fuentes, J. L., and M. J. Adang.** 2006. Cry toxin mode of action in susceptible and resistant *Heliothis virescens* larvae. J. Invertebr. Pathol. **92:**166–171.
39. **Jurat-Fuentes, J. L., and M. J. Adang.** 2006. The *Heliothis virescens* cadherin protein expressed in *Drosophila* S2 cells functions as a receptor for *Bacillus thuringiensis* Cry1A but not Cry1Fa toxins. Biochemistry **45:**9688–9695.
40. **Jurat-Fuentes, J. L., L. J. Gahan, F. L. Gould, D. G. Heckel, and M. J. Adang.** 2004. The HevCaLP protein mediates binding specificity of the Cry1A class of *Bacillus thuringiensis* toxins in *Heliothis virescens*. Biochemistry **43:**14299–14305.
41. **Knight, P. J., N. Crickmore, and D. J. Ellar.** 1994. The receptor for *Bacillus thuringiensis* CrylA(c) δ-endotoxin in the brush border membrane of the lepidopteran *Manduca sexta* is aminopeptidase N. Mol. Microbiol. **11:**429–436.
42. **Knowles, B. H., and D. J. Ellar.** 1987. Colloid-osmotic lysis is a general feature of the mechanism of action of *Bacillus thuringiensis* δ-endotoxins with different insect specificity. Biochim. Biophys. Acta **924:**507–518.
43. **Kyte, J., and R. F. Doolittle.** 1982. A simple method for displaying the hydropathic character of a protein. J. Mol. Biol. **157:**105–132.
44. **Lee, M. K., F. Rajamohan, F. Gould, and D. H. Dean.** 1995. Resistance to *Bacillus thuringiensis* CryIA δ-endotoxins in a laboratory-selected *Heliothis virescens* strain is related to receptor alteration. Appl. Environ. Microbiol. **61:**3836–3842.
45. **Lee, M. K., B. A. Young, and D. H. Dean.** 1995. Domain III exchanges of *Bacillus thuringiensis* CryIA toxins affect binding to different gypsy moth midgut receptors. Biochem. Biophys. Res. Commun. **216:**306–312.
46. **Lefranc, M. P.** 2003. IMGT, the international ImMunoGeneTics database. Nucleic Acids Res. **31:**307–310.
47. **Li, J., D. J. Derbyshire, B. Promdonkoy, and D. J. Ellar.** 2001. Structural implications for the transformation of the *Bacillus thuringiensis* δ-endotoxins from water-soluble to membrane-inserted forms. Biochem. Soc. Trans. **29:**571–577.
48. **Li, J. D., J. Carroll, and D. J. Ellar.** 1991. Crystal structure of insecticidal δ-endotoxin from *Bacillus thuringiensis* at 2.5 Å resolution. Nature **353:**815–821.
49. **Liu, X. S., and D. H. Dean.** 2006. Redesigning *Bacillus thuringiensis* Cry1Aa toxin into a mosquito toxin. Protein Eng. Des. Sel. **19:**107–111.
50. **Lu, H., F. Rajamohan, and D. H. Dean.** 1994. Identification of amino acid residues of *Bacillus thuringiensis* δ-endotoxin CryIAa associated with membrane binding and toxicity to *Bombyx mori*. J. Bacteriol. **176:**5554–5559.
51. **Luo, K., S. Sangadala, L. Masson, A. Mazza, R. Brousseau, and M. J. Adang.** 1997. The *Heliothis virescens* 170 kDa aminopeptidase functions as "receptor A" by mediating specific *Bacillus thuringiensis* Cry1A δ-endotoxin binding and pore formation. Insect Biochem. Mol. Biol. **27:**735–743.
52. **Marroquin, L. D., D. Elyassnia, J. S. Griffitts, J. S. Feitelson, and R. V. Aroian.** 2000. *Bacillus thuringiensis* (Bt) toxin susceptibility and isolation of resistance mutants in the nematode *Caenorhabditis elegans*. Genetics **155:**1693–1699.
53. **Masson, L., B. E. Tabashnik, Y. B. Liu, R. Brousseau, and J. L. Schwartz.** 1999. Helix 4 of the *Bacillus thuringiensis* Cry1Aa toxin lines the lumen of the ion channel. J. Biol. Chem. **274:**31996–32000.
54. **Morin, S., R. W. Biggs, M. S. Sisterson, L. Shriver, C. Ellers-Kirk, D. Higginson, D. Holley, L. J. Gahan, D. G. Heckel, Y. Carriere, T. J. Dennehy,**

J. K. Brown, and B. E. Tabashnik. 2003. Three cadherin alleles associated with resistance to *Bacillus thuringiensis* in pink bollworm. Proc. Natl. Acad. Sci. USA **100:**5004–5009.

55. **Morse, R. J., T. Yamamoto, and R. M. Stroud.** 2001. Structure of Cry2Aa suggests an unexpected receptor binding epitope. Structure (Cambridge) **9:**409–417.
56. **Nagamatsu, Y., S. Toda, F. Yamaguchi, M. Ogo, M. Kogure, M. Nakamura, Y. Shibata, and T. Katsumoto.** 1998. Identification of *Bombyx mori* midgut receptor for *Bacillus thuringiensis* insecticidal CryIA(a) toxin. Biosci. Biotechnol. Biochem. **62:**718–726.
57. **Nicaise, M., M. Valerio-Lepiniec, P. Minard, and M. Desmadril.** 2004. Affinity transfer by CDR grafting on a nonimmunoglobulin scaffold. Protein Sci. **13:**1882–1891.
58. **Padlan, E. A.** 1994. Anatomy of the antibody molecule. Mol. Immunol. **31:**169–217.
59. **Pardo-López, L., I. Gómez, C. Muñoz-Garay, N. Jiménez-Juarez, M. Soberón, and A. Bravo.** 2006. Structural and functional analysis of the prepore and membrane-inserted pore of Cry1Ab toxin. J. Invertebr. Pathol. **92:**172–177.
60. **Pettersen, E. F., T. D. Goddard, C. C. Huang, G. S. Couch, D. M. Greenblatt, E. C. Meng, and T. E. Ferrin.** 2004. UCSF Chimera—a visualization system for exploratory research and analysis. J. Comput. Chem. **25:**1605–1612.
61. **Pigott, C. R., and D. J. Ellar.** 2007. Role of receptors in *Bacillus thuringiensis* crystal toxin activity. Microbiol. Mol. Biol. Rev. **71:**255–281.
62. **Rajamohan, F., O. Alzate, J. A. Cotrill, A. Curtiss, and D. H. Dean.** 1996. Protein engineering of *Bacillus thuringiensis* delta-endotoxin: mutations at domain II of CryIAb enhance receptor affinity and toxicity toward gypsy moth larvae. Proc. Natl. Acad. Sci. USA **93:**14338–14343.
63. **Rajamohan, F., S. R. Hussain, J. A. Cotrill, F. Gould, and D. H. Dean.** 1996. Mutations at domain II, loop 3, of *Bacillus thuringiensis* CryIAa and CryIAb delta-endotoxins suggest loop 3 is involved in initial binding to lepidopteran midguts. J. Biol. Chem. **271:**25220–25226.
64. **Rajamohan, F., M. K. Lee, and D. H. Dean.** 1998. *Bacillus thuringiensis* insecticidal proteins: molecular mode of action. Prog. Nucleic Acid Res. Mol. Biol. **60:**1–27.
65. **Rausell, C., L. Pardo-Lopez, J. Sanchez, C. Munoz-Garay, C. Morera, M. Soberon, and A. Bravo.** 2004. Unfolding events in the water-soluble monomeric Cry1Ab toxin during transition to oligomeric pre-pore and membrane-inserted pore channel. J. Biol. Chem. **279:**55168–55175.
66. **Sangadala, S., F. S. Walters, L. H. English, and M. J. Adang.** 1994. A mixture of *Manduca sexta* aminopeptidase and phosphatase enhances *Bacillus thuringiensis* insecticidal CryIA(c) toxin binding and $^{86}Rb^{+}$-K^{+} efflux *in vitro*. J. Biol. Chem. **269:**10088–10092.
67. **Schnepf, E., N. Crickmore, J. Van Rie, D. Lereclus, J. Baum, J. Feitelson, D. R. Zeigler, and D. H. Dean.** 1998. *Bacillus thuringiensis* and its pesticidal crystal proteins. Microbiol. Mol. Biol. Rev. **62:**775–806.
68. **Schwartz, J. L., Y. J. Lu, P. Sohnlein, R. Brousseau, R. Laprade, L. Masson, and M. J. Adang.** 1997. Ion channels formed in planar lipid bilayers by *Bacillus thuringiensis* toxins in the presence of *Manduca sexta* midgut receptors. FEBS Lett. **412:**270–276.
69. **Soderlind, E., L. Strandberg, P. Jirholt, N. Kobayashi, V. Alexeiva, A. M. Aberg, A. Nilsson, B. Jansson, M. Ohlin, C. Wingren, L. Danielsson, R. Carlsson, and C. A. Borrebaeck.** 2000. Recombining germline-derived CDR sequences for creating diverse single-framework antibody libraries. Nat. Biotechnol. **18:**852–856.
70. **Stewart, G. S., K. Johnstone, E. Hagelberg, and D. J. Ellar.** 1981. Commitment of bacterial spores to germinate. A measure of the trigger reaction. Biochem. J. **198:**101–106.
71. **Tsuda, Y., F. Nakatani, K. Hashimoto, S. Ikawa, C. Matsuura, T. Fukada, K. Sugimoto, and M. Himeno.** 2003. Cytotoxic activity of *Bacillus thuringiensis* Cry proteins on mammalian cells transfected with cadherin-like Cry receptor gene of *Bombyx mori* (silkworm). Biochem. J. **369:**697–703.
72. **Vachon, V., G. Prefontaine, F. Coux, C. Rang, L. Marceau, L. Masson, R. Brousseau, R. Frutos, J. L. Schwartz, and R. Laprade.** 2002. Role of helix 3 in pore formation by the *Bacillus thuringiensis* insecticidal toxin Cry1Aa. Biochemistry **41:**6178–6184.
73. **Vachon, V., G. Prefontaine, C. Rang, F. Coux, M. Juteau, J. L. Schwartz, R. Brousseau, R. Frutos, R. Laprade, and L. Masson.** 2004. Helix 4 mutants of the *Bacillus thuringiensis* insecticidal toxin Cry1Aa display altered pore-forming abilities. Appl. Environ. Microbiol. **70:**6123–6130.
74. **Vadlamudi, R. K., T. H. Ji, and L. A. Bulla, Jr.** 1993. A specific binding protein from *Manduca sexta* for the insecticidal toxin of *Bacillus thuringiensis* subsp. *berliner.* J. Biol. Chem. **268:**12334–12340.
75. **Vaughan, T. J., A. J. Williams, K. Pritchard, J. K. Osbourn, A. R. Pope, J. C. Earnshaw, J. McCafferty, R. A. Hodits, J. Wilton, and K. S. Johnson.** 1996. Human antibodies with sub-nanomolar affinities isolated from a large non-immunized phage display library. Nat. Biotechnol. **14:**309–314.
76. **Vílchez, S., J. Jacoby, and D. J. Ellar.** 2004. Display of biologically functional insecticidal toxin on the surface of lambda phage. Appl. Environ. Microbiol. **70:**6587–6594.
77. **Ward, E. S., and D. J. Ellar.** 1983. Assignment of the delta-endotoxin gene of *Bacillus thuringiensis var. israelensis* to a specific plasmid by curing analysis. FEBS Lett. **158:**45–49.
78. **Wei, J. Z., K. Hale, L. Carta, E. Platzer, C. Wong, S. C. Fang, and R. V. Aroian.** 2003. *Bacillus thuringiensis* crystal proteins that target nematodes. Proc. Natl. Acad. Sci. USA **100:**2760–2765.
79. **Wellman-Desbiens, E., and J. C. Cote.** 2004. Screening of the insecticidal activity of *Bacillus thuringiensis* strains against *Lygus hesperus* (Hemiptera: Miridae) nymphal population. J. Econ. Entomol. **97:**251–258.
80. **Wolfersberger, M. G., P. Luethy, A. Maurer, P. Parenti, F. V. Sacchi, B. Giordana, and G. M. Hanozet.** 1987. Preparation and partial characterisation of amino acid transporting brush border membrane vesicles from the larval midgut of the cabbage butterfly (*Pieris brassicae*). Comp. Biochem. Physiol. A **86:**301–308.
81. **Wu, S. J., C. N. Koller, D. L. Miller, L. S. Bauer, and D. H. Dean.** 2000. Enhanced toxicity of *Bacillus thuringiensis* Cry3A delta-endotoxin in coleopterans by mutagenesis in a receptor binding loop. FEBS Lett. **473:** 227–232.
82. **Xie, R., M. Zhuang, L. S. Ross, I. Gómez, D. I. Oltean, A. Bravo, M. Soberón, and S. S. Gill.** 2005. Single amino acid mutations in the cadherin receptor from *Heliothis virescens* affect its toxin binding ability to Cry1A toxins. J. Biol. Chem. **280:**8416–8425.
83. **Xu, X., L. Yu, and Y. Wu.** 2005. Disruption of a cadherin gene associated with resistance to Cry1Ac δ-endotoxin of *Bacillus thuringiensis* in *Helicoverpa armigera*. Appl. Environ. Microbiol. **71:**948–954.
84. **Zemlin, M., M. Klinger, J. Link, C. Zemlin, K. Bauer, J. A. Engler, H. W. Schroeder, Jr., and P. M. Kirkham.** 2003. Expressed murine and human CDR-H3 intervals of equal length exhibit distinct repertoires that differ in their amino acid composition and predicted range of structures. J. Mol. Biol. **334:**733–749.
85. **Zeytun, A., A. Jeromin, B. A. Scalettar, G. S. Waldo, and A. R. Bradbury.** 2003. Fluorobodies combine GFP fluorescence with the binding characteristics of antibodies. Nat. Biotechnol. **21:**1473–1479.
86. **Zhang, X., M. Candas, N. B. Griko, L. Rose-Young, and L. A. Bulla, Jr.** 2005. Cytotoxicity of *Bacillus thuringiensis* Cry1Ab toxin depends on specific binding of the toxin to the cadherin receptor BT-R_1 expressed in insect cells. Cell Death Differ. **12:**1407–1416.
87. **Zhang, X., M. Candas, N. B. Griko, R. Taussig, and L. A. Bulla, Jr.** 2006. A mechanism of cell death involving an adenylyl cyclase/PKA signaling pathway is induced by the Cry1Ab toxin of *Bacillus thuringiensis*. Proc. Natl. Acad. Sci. USA **103:**9897–9902.